Material Measurements Using VNA-Based Material Characterization Kits Subject to Thru-Reflect-Line Calibration

Yi Wang, *Student Member, IEEE*, Xiaobang Shang, *Senior Member, IEEE*, Nick M. Ridler, *Fellow, IEEE*,
Mira Naftaly, Alexandros I. Dimitriadis, Tongde Huang, and Wen Wu, *Senior Member, IEEE*

***Abstract*—This article presents a study of different calibration techniques for vector network analyzer -based material measurements using commercially available material characterization kits (MCKs). Such MCKs are designed for fast broadband material characterization at millimeter-wave and terahertz frequencies and are based on gated-reflect-line calibration for removal of errors associated with the fixture. In this article, we have applied thru-reflect-line (TRL) calibration to the MCKs, yielding robust *S*-parameters that are used to calculate the relative permittivity and loss tangent of materials. Two different types of line standards, i.e., custom machined corrugated lines and air lines (a quarter-wave air gap between the ports of the MCKs), were employed to produce the desired phase shift. Both types of standard produced similar results. These investigations were carried out on three types of low-loss dielectric material, using MCKs operating at two selected waveguides bands within the range 140–750 GHz. The same samples were measured using time-domain spectroscopy (TDS) for comparison. The extracted relative permittivities and loss tangents using MCKs with TRL calibration and TDS are compared against literature values. Good agreement is achieved.**

***Index Terms*—Loss tangent, millimeter-wave measurements, relative permittivity, terahertz measurements, time-domain spectrometer (TDS), thru-reflect-line (TRL) calibration, vector network analyzer (VNA).**

I. INTRODUCTION

THERE is an increasing interest in the exploitation of the millimeter-wave and terahertz spectrum, and this has driven the demand for accurate characterization of materials properties (relative permittivity, ε', and loss tangent, tan δ) used in this frequency range. There exist different measurement methods for solid dielectric materials at millimeter-wave and terahertz frequencies, and these methods include time-domain spectroscopy (TDS) [1], [2], open resonator [3], [4], and free-space methods [5], [6] among others. TDS employs single-cycle pulse waveforms that are detected coherently in the time domain, and is capable of measuring materials over a broad frequency range (from around 100 GHz to a few THz). The open-resonator technique relies on measurements of high quality-factor (Q) resonators, with and without specimens inserted, for calculation of dielectric material properties. This technique allows precise characterization of dielectric materials (including those with very small loss tangents); however, it operates over a narrow frequency range only and requires the specimen thickness to be an integer number of half wavelengths (in the medium of the dielectric specimen). The free-space method based on a vector network analyzer (VNA) represents another mainstream approach for characterization of dielectric materials over a broad frequency range. This is a noncontact technique capable of measurement at varying temperatures. During the measurement, the specimens are placed between two corrugated antennas, which are used to launch high purity fundamental-mode Gaussian beams. Focusing elements, such as parabolic mirrors or lenses, are usually employed to reduce the waist radius of the Gaussian beam illuminating the specimens, in order to make it smaller than the lateral size of the specimen. This is to eliminate or minimize edge diffraction errors; otherwise, the required specimen size needs to be considerably large (which is often impractical). The free-space measurement method has been utilized for material characterizations at frequencies from a few GHz [7] to as high as 750 GHz [8], [9], and 1.1 THz [10].

Recently, new commercial material characterization kits (MCKs), have been developed by SWISSto12 as an alternative measurement technique. These MCKs operate in a similar way to the free-space technique, with several significant differences: first, the waves in MCKs propagate in an enclosed environment—in corrugated circular waveguides operating in the HE_{11} mode – with extremely low propagation loss; second, the whole system is compact and self-contained, eliminating the need for bulky mirrors or lenses. Fig. 1 shows a WR-5 band (140–220 GHz) MCK system at National Physical Laboratory (NPL).

Manuscript received January 27, 2020; revised April 23, 2020; accepted May 27, 2020. Date of publication June 3, 2020; date of current version September 2, 2020. This work was supported by the European Metrology Programme for Innovation and Research (EMPIR) Project 18SIB09 “Traceability for electrical measurements at millimetre-wave and terahertz frequencies for communications and electronics technologies”. The EMPIR Programme is co-financed by the participating states and from the European Union’s Horizon 2020 Research and Innovation Programme. *(Corresponding authors: Xiaobang Shang; Nick M. Ridler.)*

Yi Wang, Tongde Huang, and Wen Wu are with the Ministerial Key Laboratory of JGMT, Nanjing University of Science and Technology, Nanjing 210094, China (e-mail: wangyi@njust.edu.cn; tongdeh@njust.edu.cn; wuwen@njust.edu.cn).

Xiaobang Shang, Nick M. Ridler, and Mira Naftaly are with the National Physical Laboratory, Teddington TW11 0LW, U.K. (e-mail: xiaobang.shang@npl.co.uk; nick.ridler@npl.co.uk; mira.naftaly@npl.co.uk).

Alexandros I. Dimitriadis is with Swissto12 SA, CH-1020 Renens, Switzerland (e-mail: a.dimitriades@swissto12.ch).

Color versions of one or more of the figures in this article are available online at https://ieeexplore.ieee.org.

Digital Object Identifier 10.1109/TTHZ.2020.2999631

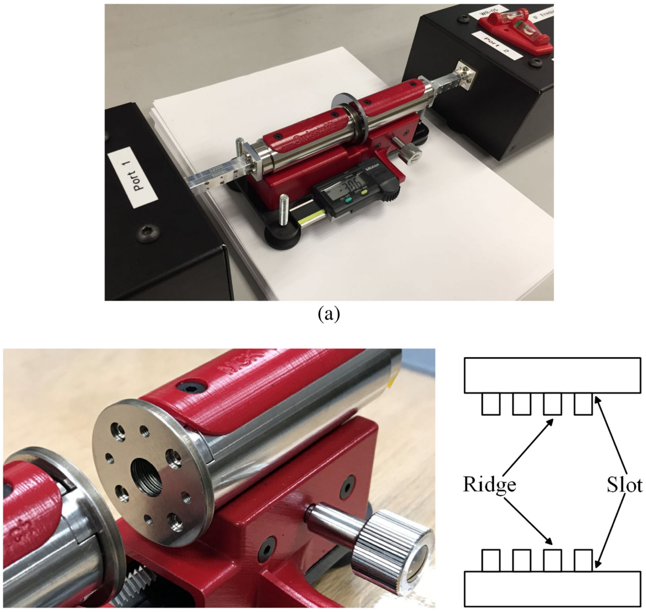

(a)

(b)

(c)

Fig. 1. (a) Overview of the system comprised of a WR-5 (140–220 GHz) MCK and a pair of WR-5 VNA frequency extender heads that are connected to a Keysight PNA-X in-operando at NPL. A silicon plate is shown sandwiched between the two corrugated waveguides of the MCK. (b) Close-up view of the corrugated waveguides/antennas while the two MCK ports are separated. (c) Diagram illustrating the corrugated waveguides. This drawing is not to scale.

During measurement, the MCK is attached to a VNA, which measures the *S*-parameters of the material under test (MUT) in the frequency domain. MCKs are typically calibrated to the end of the corrugated waveguides using the gated-reflect-line (GRL) technique [11], [12].

Thru-reflect-line (TRL) [13]–[15] is a very accurate and reliable two-port calibration technique that has been used extensively for VNA calibrations. TRL calibration does not require reflect standards with known reflections as long as the reflect standards are identical on both ports [15]. TRL calibration is most often performed when a high level of accuracy is required, since the calibration standards do not need to be defined as completely and accurately as required by other calibration techniques. Thus, TRL calibration is widely applied to waveguide and planar measurements within the millimeter-wave and terahertz frequency bands. In this work, the TRL technique has been applied to the calibration of MCKs, so that more accurate *S*-parameter measurements of the MUT can be obtained. These *S*-parameters were then employed to calculate the relative permittivity and loss tangent of materials. Time gating was utilized to remove the multiple reflections within the corrugated waveguides and at the interfaces. Two different types of line standards, i.e., custom machined corrugated lines and air lines (using an air gap between the ports of the MCK), were utilized to produce the required electrical delays. An investigation of measurements using MCK with TRL calibration was carried out on three types of dielectric materials (PTFE, silicon, and Rogers 3003), using MCKs operating in the WR-5 band and the WM-380 band (500–750 GHz). The same samples were measured using a well-established TDS system at NPL, for benchmarking the measurement results.

To the best of the authors' knowledge, this is the first time that TRL calibration has been applied to remove the errors associated with MCKs. The line standard based on an air gap is also demonstrated to be an effective and simple approach for implementing TRL calibration, without the need for additional components. Wang *et al.* [16] reported on the characterization of several dielectric materials in the WR-15 band (50–75 GHz) using a MCK with default GRL calibration, and the extracted results show good agreement with published literature values after measurement uncertainties are taken into account. Here, the work is extended further, in terms of utilization of a more robust TRL calibration technique for the MCK; measurement of materials over two different waveguide bands within the range of 140–750 GHz so that a broader study is possible; and direct comparison of results from MCKs and TDS.

The article is organized as follows: in Section II, the experimental setup and calibration technique are introduced; Section III describes the measurement results for the abovementioned dielectric samples using MCKs and TDS; followed by conclusion in Section IV.

II. MATERIAL MEASUREMENTS USING MCKS

A. *Measurement System*

Fig. 1(a) shows the WR-5 band material characterization setup, which is comprised of a WR-5 MCK, a pair of VDI WR-5 frequency extenders, and a Keysight N5247 PNA-X network analyzer (not shown). Fig. 1(b) shows a close up of the corrugated waveguides of the WR-5 MCK. Corrugations are added to the inner wall of the circular waveguide to produce an HE_{11} mode (a combination of TE_{11} and TM_{11} modes) that has low propagation loss within waveguide and the ability to launch a high purity Gaussian beam. The diameters of the ridges and slots of the corrugated waveguide are 8.200 mm and 9.052 mm, respectively. The input of this MCK is a standard WR-5 rectangular waveguide, which is coupled to the corrugated waveguide via a smooth-walled circular waveguide and a corrugated conical horn antenna.

The MCK can be directly connected to the frequency extenders due to its standard waveguide flanges. To measure a dielectric material, the sample is placed in the gap between the two corrugated waveguides, where a gap adjustment mechanism is used to open and close the MCK. *S*-parameter measurements are performed following calibration, the details of which are described in the following section.

Two different sets of MCKs were employed for measurements over the following waveguide bands: WR-5 and WM-380. The investigation was carried out at selected waveguide bands, corresponding to the VNA frequency coverage at NPL. In these measurements, the VNA was set to measure at 2001 frequency points with an intermediate frequency (IF) bandwidth of 50 Hz. No averaging was applied to the data. Three different types of common dielectric materials, i.e., PTFE (thickness 5.99 mm), silicon (thickness 3.06 mm), and Rogers 3003 (thickness 1.50 mm), were measured. The PTFE sample was machined in-house from a rod to have a thickness of 5.99 mm. This relatively large thickness facilitates the measurement of loss tangent, since PTFE is a relatively low-loss material. The silicon sample was obtained from Tydex, and its grade is high-resistivity float zone silicon. The Rogers 3003 sample is based on ceramic-filled PTFE composites, designed by manufacturer for its low dielectric loss at high frequencies. All measurements were taken at the ambient laboratory temperature of 23 °C ± 1 °C. The silicon sample was measured in the dark, due to its photoconductive nature.

Time-domain gating is usually applied to free-space measurement to separate the desired signal from spurious reflections generated elsewhere in the measurement system or within the sample. Briefly, a bandpass window is implemented in time domain such that any signals outside of the region of interest are discarded (i.e., assigned to be zero). Then, the processed time-domain signal is converted to the frequency domain, and the gated *S*-parameters are utilized to calculate the material properties. In this work, the time-domain gating was carried out on the VNA, using a Kaiser–Bessel window function [17]. The optimum gate width depends on the characteristics of the MUT and on the operating frequencies. Minimizing the gate width can minimize the ripple generated by undesired multipath signals. However, systematic errors in the extracted material properties will be introduced if the gate width is smaller than the width of the desired signal [7]. Also, it is recommended that MCKs use time-domain gating, and the gate width is usually specified as 400 ps [11]. In practice, the optimum gate width varies with the characteristics of the measured specimen and can be calculated from the approximate permittivity, sample thickness, and the operating frequency [18]. In this work, the time-gating width for PTFE, silicon, and Rogers 3003 was calculated to be 280 ps, 800 ps, and 120 ps, respectively. The variation of frequency only results in a small difference in the corresponding gate width, and therefore a single value calculated using the midband frequency has been specified.

In this work, time-domain gating was applied to eliminate reflections associated with the MCK fixtures and test equipment. The sidelobes occurring due to multiple reflections inside the sample were contained within the gating window. Multiple reflections in the sample were taken into account since they constitute part of the physical response of the MUT. Therefore, the formulas for reflection and transmission of a wave propagating through a dielectric slab are consistent with the *S*-parameters measured by the system.

B. Comparison of Calibration Techniques

The default calibration technique for the MCK system is the GRL, which is carried out at the end of the corrugated waveguides prior to making measurements of *S*-parameters. The GRL method requires a simple zero-length thru standard and a metallic reflecting plate as the reflect standard [11]. TRL calibration offers high accuracy and needs only minimal knowledge of the electrical behavior of the standards used; hence, it was employed in this work to calibrate the MCKs to the reference planes at the end of the corrugated waveguides. The thru standard is realized by closing the gap to join the two halves of the corrugated waveguides. The reflect standard is realized by placing a short circuit (a 1 mm thick metal shim, provided with the MCK) between the two halves of the corrugated waveguides.

Fig. 2. Photograph of the machined line standards for the WR-5 band MCK. Both lines have the same thickness of 0.420 mm. The diameters of the inner holes are 9.052 mm and 8.200 mm.

For the WR-5 MCK, two different types of line standards, i.e., custom machined metal lines, and an airline (effectively an air gap between the corrugated waveguides of the MCK), were employed to produce the required phase shift for TRL calibration. Fig. 2 shows two machined line standards with diameters of 8.200 mm and 9.052 mm. These correspond to the ridge and slot diameters, respectively. The former introduces no change in the diameter of the transmission line when the line standard is sandwiched between the two ports, whereas the latter represents the case where the corrugated waveguide is continued. Ideally, the length of line standards should be a quarter wavelength (in the transmission lines), which can be calculated by following the procedure in [19]. The diameter of the ridge has been used in the calculation. The wavenumber of vacuum, *k*, and the cut-off wavenumber of a corrugated waveguide, k_c, can be expressed as

$$k = \omega\sqrt{\mu_0\varepsilon_0} \tag{1}$$

$$k_c = \frac{2.405}{a} \tag{2}$$

where ω is the center angular frequency of the waveguide band, ε_0 and μ_0 are the permittivity and permeability of vacuum, and a is the radius of the ridge. The propagation constant of the corrugated waveguide, β, is given by

$$\beta = \sqrt{k^2 + {k_c}^2}. \tag{3}$$

The wavelengths in the corrugated waveguide ($\lambda_{\text{waveguide}}$) and in free space ($\lambda_{\text{freespace}}$), are given by the following equations:

$$\lambda_{\text{waveguide}} = \frac{2\pi}{\beta} \tag{4}$$

$$\lambda_{\text{freespace}} = \frac{c}{f} \tag{5}$$

TABLE I

PHYSICAL DIMENSIONS OF CORRUGATED WAVEGUIDES OF MCKS AND CALCULATED QUARTER WAVELENGTH FOR MIDDLE BAND FREQUENCY

	WR-5	WM-380
Mid-band frequency (GHz)	180	625
Ridge diameter (mm)	8.200	5.000
Slot diameter (mm)	9.052	5.250
$\lambda/4$ corrugated waveguide (mm)	0.422	0.120
$\lambda/4$ free-space (mm)	0.416	0.120
Air gap length used (mm)	0.420	0.120

where c is the speed of light in vacuum and f is the center frequency of the waveguide band, $\omega = 2\pi f$. Table I gives the calculated desired lengths, at the center frequency of the waveguide band, for both metal line standards and air gaps. These two lengths are very close to each other, demonstrating that the wave propagates in the corrugated waveguide in a similar fashion as in free space. The length values for the standards used are rounded to two decimal places due to the limited accuracy of the length measurement. This has negligible effect on the TRL calibration, since only an approximate length is required by the TRL calibration algorithm.

Table I also shows the dimensions of the corrugated waveguides for the MCKs operating in the WM-380 band. For this MCK, no metal line standards have been fabricated, and only a line standard based on an air gap was employed for TRL calibration in this band. The length of this standard is given in Table I.

III. RESULTS

Three different common dielectric materials (PTFE, silicon, and Rogers 3003) were measured using the MCK with different calibration techniques in the two waveguide bands within the range of 140–750 GHz. The same samples were also measured using TDS for comparison. The TDS system used was a laboratory-built instrument employing a standard configuration incorporating a Ti:Sapphire femtosecond laser, four off-axis parabolic mirrors, a biased GaAs emitter, and electro-optic detection using a ZnTe crystal and balanced Si photodiodes. The TDS was frequency calibrated and had its amplitude linearity verified as described in [20].

The permittivity and loss tangent of the materials can be calculated directly from the S-parameters obtained using MCKs. In this work, the National Institute of Standards and Technology (NIST) precision model [21] was employed to extract the material properties from S_{21} (or S_{12}). The reflection responses, S_{11} (or S_{22}), were not used for calculation. This is a common approach used in free-space based techniques, in that the reflection responses are more prone to errors. To reduce random errors, the MCK measurements were repeated six times, and the results reported below are the mean of these six repetitions.

A. *Comparison of Calibration Techniques in the WR-5 Band*

Four different calibrations were applied to the WR-5 MCK and these calibrations are: GRL, TRL using the metal line standard with a larger inner diameter, TRL using the metal line standard with a smaller inner diameter, TRL using an air gap as the line standard. These metal line standards are shown in Fig. 2.

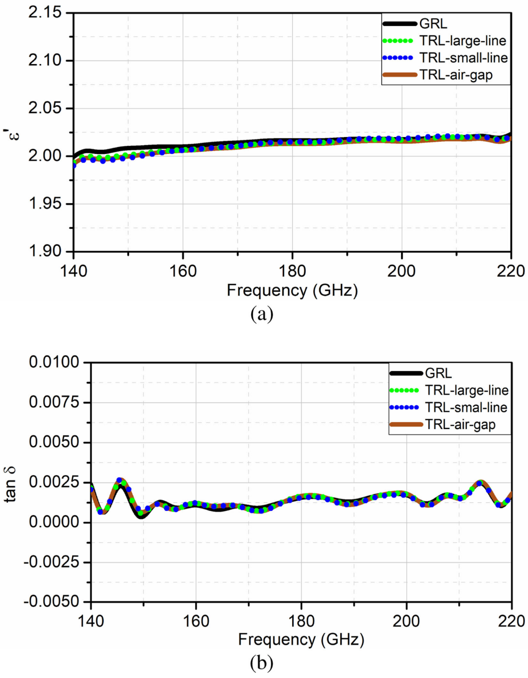

(a)

(b)

Fig. 3. (a) Extracted relative permittivity, ε'. (b) Loss tangent, tan δ, for the PTFE sample (thickness 5.99 mm) using the WR-5 MCK with four different calibration techniques: GRL, TRL using metal line standard with a larger inner diameter, TRL using metal line standard with a smaller inner diameter, TRL using an air gap as a line standard.

As abovementioned in Section II, all TRL calibrations were also subject to gating in the time domain. The gate widths were optimized for each sample. Figs. 3, 4, and 5 show the extracted relative permittivities and loss tangents for the PTFE, silicon, and Rogers 3003 samples, respectively. These three MUTs are homogeneous materials, and therefore should have a weak and monotonous frequency dependence. Hence, traces with no oscillations are expected. The relative permittivities and loss tangents extracted using TRL calibrations have smoother traces, particularly for the silicon sample which has a relatively high relative permittivity. In contrast, there exist noticeable ripples in the measured results of the silicon sample subject to GRL calibration. The observed oscillations in the data are believed to be due to standing waves in the sample and mismatches associated with the MCK. TRL provides improved and more robust correction to errors in the measurements, compared to GRL (which is an inherently simpler calibration technique [12]). This is reflected in the measured relative permittivity and loss tangent of the silicon sample, where TRL calibration yields considerable improvement (in terms of the reduced size of the ripples) compared with GRL, as shown in Fig. 4(b). The improvement is less obvious for the PTFE and Rogers 3003 samples, due to their relatively low relative permittivities (i.e., the small amount of energy reflected from the samples and subsequent insignificant multiple reflections).

TRL calibrations based on different line standards produce similar results, as shown in Figs. 3–5. This suggests that a simple

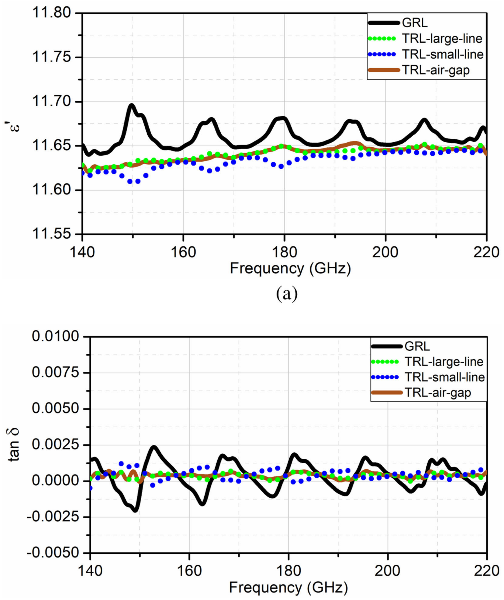

(a)

(b)

Fig. 4. (a) Extracted relative permittivity, ε'. (b) Loss tangent, tan δ, for the silicon sample (thickness 3.06 mm) using MCK with four different calibration techniques: GRL, TRL using metal line standard with a larger inner hole, TRL using metal line standard with a smaller inner hole, TRL using an air gap as a line standard.

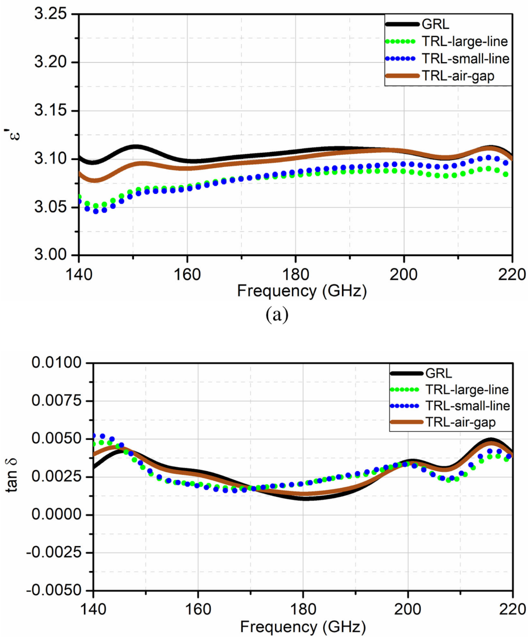

(a)

(b)

Fig. 5. (a) Extracted relative permittivity, ε'. (b) Loss tangent, tan δ, for Rogers 3003 sample (thickness 1.50 mm) using MCK with four different calibration techniques: GRL, TRL using metal line standard with larger inner hole, TRL using metal line standard with smaller inner hole, TRL using an air gap as a line standard.

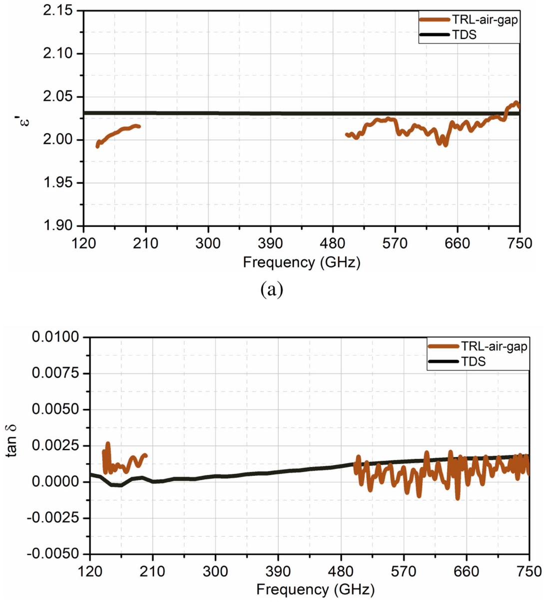

(a)

(b)

Fig. 6. (a) Extracted relative permittivity, ε'. (b) Loss tangent, tan δ, for the PTFE sample (thickness 5.99 mm) using MCK with TRL-air-gap calibration and TDS.

air gap can work as effectively as dedicated lines fabricated from metal, due to the fact that the HE_{11} mode in the corrugated waveguide couples to the fundamental Gaussian mode at the aperture with very high efficiency (i.e., around 98 %) [11], [22].

The results for Rogers 3003 show some differences between these four calibration techniques. This is believed to be related to the small sample thickness, making the sample more prone to deformation during measurement. As described abovementioned, samples are clamped between the two corrugated waveguides of the MCK, and a sufficient contact force needs to be applied to avoid any air gaps. For thin samples, the sample can become slightly distorted during measurement, which introduces errors in the measurement results because the MCK technique (like the conventional free-space technique) assumes plane-wave illumination of the samples [23]. The deviation in results achieved using different calibration techniques, as shown in Fig. 5, is likely attributed to such measurement errors, instead of the different calibration techniques.

Additionally, there is a significant possibility that there may be sidelobes and multiple reflections present at the corrugated horn measurement reference planes. This will introduce errors that will not be fully corrected by the calibration process. These errors will therefore need to be accounted for, during an evaluation of the overall uncertainty in these measurements.

B. Comparison Between MCK and TDS

The same three samples were also measured using a MCK, calibrated with the TRL technique (based on an air gap as a line standard), in the WM-380 waveguide band. These results were compared with those from TDS measurements carried out at NPL. Figs. 6, 7, and 8 show the extracted relative permittivities and loss tangents for PTFE, silicon, and Rogers 3003, respectively. The results using MCK show reasonable agreement with those obtained by TDS. Note that the MCKs' results of each sample were a combination of two separate measurement exercises involving different hardware: hence, random errors

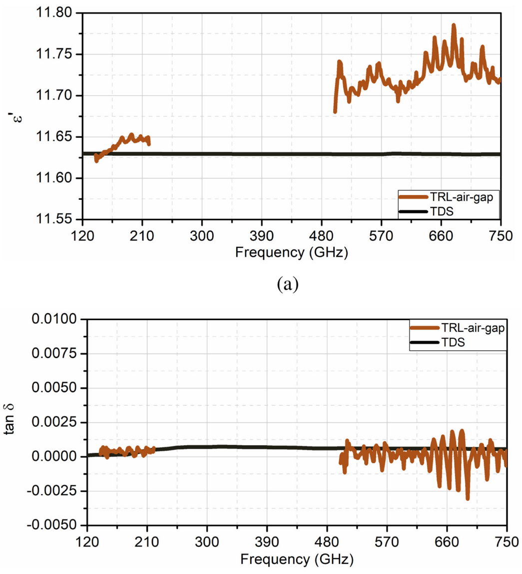

(a)

(b)

Fig. 7. (a) Extracted relative permittivity, ε'. (b) Loss tangent, $\tan\delta$, for the silicon sample (thickness 3.06 mm) using MCK with TRL-air-gap calibration and TDS.

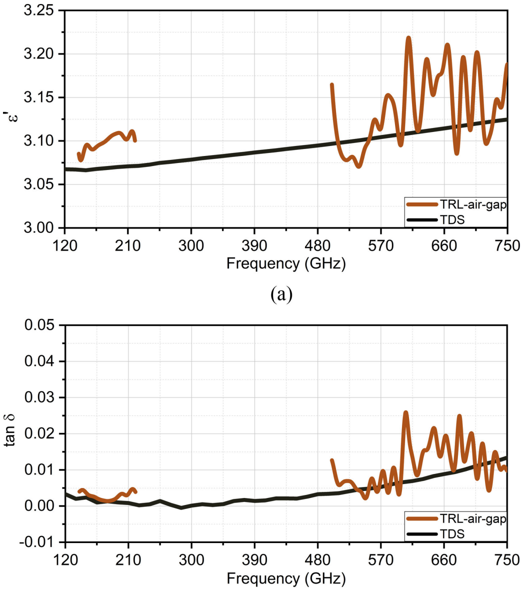

(a)

(b)

Fig. 8. (a) Extracted relative permittivity, ε'. (b) Loss tangent, $\tan\delta$, for Rogers 3003 sample (thickness 1.50 mm) using MCK with TRL-air-gap calibration and TDS.

TABLE II

EXTRACTED RELATIVE PERMITTIVITY VALUES USING MCK WITH TRL-AIR-GAP CALIBRATION, COMPARED WITH TDS VALUES, AVERAGED OVER FREQUENCY

Samples	TRL using an air gap as line standard, ε'	TDS, ε'	Literature, ε'
PTFE	2.014	2.030 ± 0.010	2.060 @ 300 GHz, [24] 2.040 @ 500 GHz, [25]
Silicon	11.683	11.630 ± 0.010	11.700 @ 700 GHz, [26] 11.670 @ 1 THz, [27]
Roger 3003	3.117	3.100 ± 0.010	3.000 @ 60 GHz, [28] 3.000 @ 10 GHz, [29]

Values found in the literature are also included for comparison.

TABLE III

EXTRACTED LOSS TANGENT VALUES USING MCK WITH TRL-AIR-GAP CALIBRATION, COMPARED WITH TDS VALUES, AVERAGED OVER FREQUENCY

Samples	TRL using an air gap as line standard, tan δ	TDS, tan δ	Literature, tan δ
PTFE	0.001 0	0.001 0 ± 0.000 10	0.002 0 @ 300 GHz, [24] 0.002 4 @ 500 GHz, [25]
Silicon	0.000 3	0.000 5 ± 0.000 03	0.000 3 @ 700 GHz, [26] 0.000 4 @ 1 THz, [27]
Rogers 3003	0.007 0	0.005 8 ± 0.000 60	0.001 3 @ 60 GHz, [28] 0.001 3 @ 10 GHz, [29]

Values found in the literature are also included for comparison.

such as contact repeatability have contributed to the variability in these results. The TDS measurement captured the data for each sample in one go and therefore is not expected to vary due to crossing different waveguide bands. This is believed to account for some of the observed differences in the results from MCK and TDS.

The measured loss tangent shown in Figs. 4, 6, and 7 include some values that are less than zero. Although it is theoretically not possible for the true value of the loss tangent of these materials to be less than zero, in practice, such measured values can sometimes occur for very low-loss materials (i.e., where the true value of the loss tangent is close to zero), due to inherent measurement error. If this error is negative, the measured value will be less than the true value, which can result in measured values being less than zero.

It can be observed from Fig. 7(b) that periodic oscillation occurs in the measured loss tangent of the silicon sample, with an etalon frequency of around 15 GHz. This is attributable to the standing waves in the silicon sample, which cannot be eliminated by calibration techniques. The etalon frequency, which is a function of sample thickness, L, and material refractive index, n (i.e., $\sqrt{\varepsilon'}$), can be calculated as $c/(2nL)$. Similarly, oscillations occur in the result of the PTFE sample (see Fig. 6), with an etalon frequency of 17.5 GHz. This oscillation is weaker due to the refractive index of PTFE being significantly lower than silicon, resulting in oscillations with smaller amplitudes. The oscillation shown in Fig. 8 is likely caused by factors including standing waves in the Rogers 3003 sample and unexpected multiple reflections (e.g., as a result of sample deformation during measurement).

Tables II and III summarize the results extracted using MCKs and TDS. Note that the loss tangent of Rogers 3003, which is a lossy material, increases with frequency. Therefore, in this case the values of relative permittivity and loss tangent obtained by MCK are averaged over two waveguide bands within the frequency range of 140–750 GHz and the values obtained by TDS are averaged over the frequency range of 120–750 GHz. The quoted values for TDS include estimates of the overall uncertainties of these measurements. Wang *et al.* [16] present an investigation into measurement uncertainties in the extracted material properties associated with MCKs, due to random errors (i.e., the samples' insertion repeatability) and systematic errors (i.e., measured *S*-parameters and thickness of samples). It has been found that systematic errors account for most of the overall uncertainties [16]. Here, this work is devoted to an investigation into new calibration techniques for MCKs, and so uncertainties are not discussed.

The values of relative permittivity and loss tangent presented in Tables II and III also show acceptable agreement with those published in the literature. It is noted that there are no published values for Rogers 3003 at higher frequencies (i.e., greater than 100 GHz) and that values at higher frequencies are expected to be different from values at lower frequencies since Rogers 3003 is a polar material with significant absorption.

IV. CONCLUSION

This article has presented a study of different calibration techniques for material characterization at millimeter-wave and terahertz frequencies using MCKs. Common low-loss dielectric materials (PTFE, silicon, and Rogers 3003) have been measured using MCKs with TRL calibration techniques. Improvement in the extracted relative permittivity and loss tangent has been achieved via the TRL calibrations. It has been demonstrated that TRL calibration can adopt an air gap as the line standard. This is beneficial to users as no additional hardware is required to implement the TRL technique and to achieve higher accuracy in the measurements. The results from MCKs have also been benchmarked with TDS at NPL for these three types of material. Good agreement between relative permittivity results has been obtained. Neither MCK nor TDS is ideally suited to characterize the loss tangent of very low-loss dielectric materials (such as those measured in this work). Other resonator-based techniques should provide better loss tangent measurements. In summary, MCKs with TRL calibrations have been shown to be a promising alternative technique for material characterization at millimeter-wave and terahertz frequencies.

REFERENCES

[1] M. Naftaly and R. E. Miles, "Terahertz time-domain spectroscopy for material characterization," *Proc. IEEE*, vol. 95, no. 8, pp. 1658–1665, Aug. 2007.

[2] R. Gente *et al.*, "Quality control of sugar beet seeds with thz time-domain spectroscopy," *IEEE Trans. Terahertz Sci. Technol.*, vol. 6, no. 5, pp. 754–756, Sep. 2016.

[3] B. B. Yang *et al.*, "A high-Q terahertz resonator for the measurement of electronic properties of conductors and low-loss dielectrics," *IEEE Trans. Terahertz Sci. Technol.*, vol. 2, no. 4, pp. 449–459, Jul. 2012.

[4] H. Suzuki and T. Kamijo, "Millimeter-wave measurement of complex permittivity by perturbation method using open resonator," *IEEE Trans. Instrum. Meas.*, vol. 57, no. 12, pp. 2868–2873, Dec. 2008.

[5] J. Hammler, A. J. Gallant, and C. Balocco, "Free-space permittivity measurement at terahertz frequencies with a vector network analyzer," *IEEE Trans. Terahertz Sci. Technol.*, vol. 6, no. 6, pp. 817–823, Nov. 2016.

[6] T. Tosaka, K. Fujii, K. Fukunaga, and A. Kasamatsu, "Development of complex relative permittivity measurement system based on free-space in 220–330-GHz range," *IEEE Trans. Terahertz Sci. Technol.*, vol. 5, no. 1, pp. 102–109, Jan. 2015.

[7] J. W. Schultz, *Focused Beam Methods: Measuring Microwave Materials in Free Space*. Scotts Valley, CA, USA: Create Space, 2012.

[8] T. Rubrek *et al.*, "Characterization of materials in the 50–750 GHz range using a scatterometer," in *Proc. 43rd Int. Conf. Infrared, Millimeter, Terahertz Waves*, 2018, pp. 1–2.

[9] C. Cappellin, P. H. Nielsen, R. Appleby, R. Wylde, and E. Saenz, "Detailed design and RF analysis of a scatterometer for material characterization in the 50–750 GHz range," in *Proc. 12th Eur. Conf. Antennas Propag.*, 2018, pp. 1–5.

[10] D. K. George, A. Charkhesht, and N. Q. Vinh, "New terahertz dielectric spectroscopy for the study of aqueous solutions," *Rev. Sci. Instrum.*, vol. 86, no. 12, Dec. 2015, Art. no. 123105.

[11] A. Dimitriades and R. Divorne, "MCK User Guide—Version 1.1," Swissto12 SA, Renens, Switzerland, Tech. Rep. Swissto12, 2018.

[12] P. G. Bartley and S. B. Begley, "Improved free-space S-parameter calibration," in *Proc. IEEE Instrum. Meas. Technol. Conf. Proc.*, Ottawa, ON, Canada, May 2005, pp. 372–375.

[13] S. Fregonese *et al.*, "Comparison of on-wafer TRL calibration to ISS SOLT calibration with open-short de-embedding up to 500 GHz," *IEEE Trans. Terahertz Sci. Technol.*, vol. 9, no. 1, pp. 89–97, Jan. 2019.

[14] "Agilent network analysis applying the 8510 TRL calibration for non-coaxial measurements," Agilent Technol., Santa Clara, CA, USA, Product Note 8510-8A, 2001.

[15] G. F. Engen and C. A. Hoer, "Thru-reflect-line: An improved technique for calibrating the dual six-port automatic network analyzer," *IEEE Trans. Microw. Theory Techn.*, vol. 27, no. 12, pp. 987–993, Dec. 1979.

[16] Y. Wang, X. Shang, N. Ridler, T. Huang, and W. Wu, "Characterization of dielectric materials at WR-15 band (50–75 GHz) using VNA-based technique," *IEEE Trans. Instrum. Meas.*, vol. 69, no. 7, pp. 4930–4939, Jul. 2020.

[17] Keysight Technologies Application Note, "Time domain analysis using a network analyzer," Dec. 2017. [Online]. Available: https://www.keysight.com/gb/en/assets/7018-01451/application-notes/5989-5723.pdf

[18] A. Amiet, "Free space permittivity and permeability measurements at microwave frequencies," Ph.D. dissertation, Dept. Elect. Eng., Monash Univ., Clayton, VIC, Australia, 2003.

[19] D. M. Pozar, "Transmission lines and waveguides," in *Microwave Engineering*, 4th ed., Hoboken, NJ, USA: Wiley, 2011, ch.3, pp. 96–130.

[20] M. Naftaly and R. Dudley, "Linearity calibration of amplitude and power measurements in terahertz systems and detectors," *Opt. Lett.*, vol. 34, no.5, pp. 674–676, 2009.

[21] J. Baker-Jarvis, E. J. Vanzura, and W. A. Kissick, "Improved technique for determining complex permittivity with the transmission/reflection method," *IEEE Trans. Microw. Theory Techn.*, vol. 38, no. 8, pp. 1096–1103, Aug. 1990.

[22] R. J. Wylde, "Millimetre-wave gaussian beam-mode optics and corrugated feed horns," *IEE Proc. H Microw., Opt. Antennas*, vol. 131, no. 4, pp. 258–262, Aug. 1984.

[23] R. N. Clarke *et al.*, "A guide to the characterisation of dielectric materials at RF and microwave frequencies," Inst. Meas. Control, Nat. Phys. Lab., Teddington, U.K., 2003.

[24] T. Chang, X. Zhang, X. Zhang, and H. L. Cui, "Accurate determination of dielectric permittivity of polymers from 75 GHz to 16 THz using both S-parameters and transmission spectroscopy," *Appl. Opt.*, vol. 57, no. 21, 2018, Art. no. 6032.

[25] Y.-S. Jin, G.-J. Kim, and S.-G. Jeon, "Terahertz dielectric properties of polymers," *J. Korean Phys. Soc.*, vol. 49, pp. 513–517, 2006.

[26] K. Zhou *et al.*, "Dielectric constant and loss tangent of silicon at 700–900 GHz at cryogenic temperature," *IEEE Microw. Wireless Compon. Lett.*, vol. 29, no. 7, pp. 501–503, Jul. 2019.

[27] P. H. Bolivar *et al.*, "Measurement of the dielectric constant and loss tangent of high dielectric-constant materials at terahertz frequencies," *IEEE Trans. Microw. Theory Techn.*, vol. 51, no. 4, pp. 1062–1066, Apr. 2003.

[28] C. Vázquez, S. V. Hoeye, F. L. Heras, M. Fernandez, and F. L. Heras, "Frequency scanning probe for microwave imaging," in *Proc. IEEE Antennas Propag. Soc. Int. Symp.*, Toronto, ON, Canada, 2010, pp. 1–4.

[29] P. I. Dankov, "Dielectric anisotropy of modern microwave substrates," *Microwave and Millimeter Wave Technologies from Photonic Bandgap Devices to Antenna and Applications*, Igor Minin, Ed. Rijeka, Croatia: InTech, 2010.

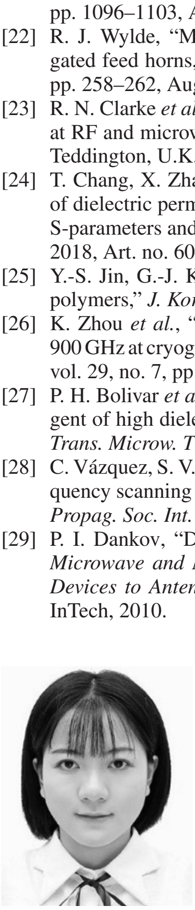

Yi Wang (Student Member, IEEE) received the B.Eng. degree from Anqing Normal University, Anqing, China, in 2016. She is currently working toward the Ph.D. degree with the Nanjing University of Science and Technology, Nanjing, China.

From January 2019 to July 2019, she was a Visiting Researcher with the Department of Electromagnetic and Electrochemical Technologies, National Physical Laboratory, Teddington, U.K., where she was involved in high-frequency electromagnetic measurement. Her current research interests include radio frequency integrated circuits, microwave passive device, and microwave measurement.

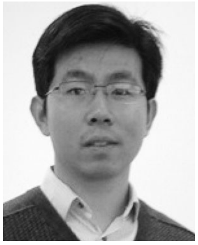

Xiaobang Shang (Senior Member, IEEE) received the B.Eng. degree (First Class) in electronics and communication engineering from the University of Birmingham, Birmingham, U.K., in 2008, the B.Eng. degree in electronics and information engineering from the Huazhong University of Science and Technology, Wuhan, China, in 2008, and the Ph.D. degree in microwave engineering from the University of Birmingham in 2011.

He is currently a Senior Research Scientist with the National Physical Laboratory, Teddington, U.K. He has authored or coauthored more than 70 scientific articles on microwave measurements and microwave circuits. Dr. Shang was the recipient of several prestigious awards, including the ARFTG Microwave Measurement Student Fellowship Award in 2009, the IEEE Tatsuo Itoh Award in 2017, and the ARMMS Steve Evans-Pughe Prize in 2017. He has been serving as the Associate Editor for the IEEE MICROWAVE AND WIRELESS COMPONENTS LETTERS, since 2020.

Nick M. Ridler (Fellow, IEEE) received the B.Sc. degree from King's College London, University of London, London, U.K., in 1981.

He is currently the Head of Science with the Department of Electromagnetic and Electrochemical Technologies, the UK's National Physical Laboratory, Teddington, U.K. He is also a Visiting Professor with the Universities of Leeds, Liverpool and Surrey, U.K., and a Nonexecutive Director of LA Techniques Ltd, Surbiton U.K. His main area of interest is precision high-frequency electromagnetic measurement (from 1 kHz to 1 THz).

He is a Fellow of the Institution of Engineering and Technology (IET) and a Fellow of the Institute of Physics (IOP). He has almost 40 years' experience working in industrial, government, and academic research establishments.

Mira Naftaly is a Physicist and Spectroscopist who has been working in the field of THz measurements, since 2002. She is currently a Senior Research Scientist with the National Physical Laboratory, Teddington, U.K. Her research interests include THz metrology, materials spectroscopy, and communications.

Alexandros I. Dimitriadis was born in Larissa, Greece, in 1985. He received the M.Sc. and Ph.D. degrees in electrical and computer engineering from the Aristotle University of Thessaloniki, Thessaloniki, Greece, in 2008 and 2013, respectively.

In 2014, he joined the Swiss Federal Institute of Technology in Lausanne, Switzerland, as a Postdoctoral Researcher and is currently with SWISSto12 as an RF Project Manager. He is also passionate about material characterization and is currently the Product Manager of the Material Characterization Kit (MCK), a commercial test fixture capable of measuring dielectric properties of materials from 25 GHz to 1.1 THz as part of a table-top, VNA-based system. His current research interests lie in the fields of passive, waveguide-based RF components such as waveguides, antennas, and filters, with an emphasis on devices that can be fabricated using novel additive manufacturing technologies.

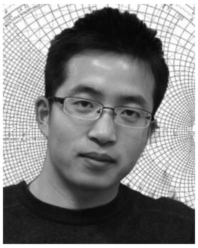

Tongde Huang received the Ph.D. degree from the Department of Electronics and Computer Engineering, The Hong Kong University of Science and Technology, Hong Kong, in 2013.

From 2014 to 2017, he was with the Microwave Electronics Laboratory Group, Chalmers University of Technology, Gothenburg, Sweden. He is currently with the Nanjing University of Science and Technology, Nanjing, China.

Wen Wu (Senior Member, IEEE) received the Ph.D. degree in electromagnetic field and microwave technology from Southeast University, Nangjing, China, in 1997.

He is currently a Professor with the School of Electronic and Optical Engineering, Nanjing University of Science and Technology, Nanjing, China. He holds 14 patents. He has authored or coauthored more than 240 journal articles and conference papers. His current research interests include microwave and millimeter-wave theories and technologies, microwave and millimeter-wave detection, and multimode compound detection. Dr. Wu was the recipient of six times of Ministerial- and Provincial-Level Science and Technology Awards.